

Article

# Experimental Study on Mechanical Properties of Marine Mud Slurry Treated by Flocculation-Solidification-High Pressure Filtration Combined Method

Chao Han <sup>1</sup>, Hongping Xie <sup>1</sup>, Bin Bai <sup>1</sup>, Rongjun Zhang <sup>2,\*</sup>, Yingchao Gao <sup>2,\*</sup> and Zhekun Zhao <sup>2</sup>

<sup>1</sup> Construction Branch of State Grid Jiangsu Electric Power Co., Ltd., Nanjing 210000, China

<sup>2</sup> School of Civil Engineering, Wuhan University, Wuhan 430072, China

\* Correspondence: ce\_zhangrj@whu.edu.cn (R.Z.); ycg1995@whu.edu.cn (Y.G.)

**Abstract:** For the massive quantities and negative impacts of dredged mud slurry, its disposal and utilization have become one of the most noticeable issues in the world. In this paper, the flocculation-solidification-high pressure filtration combined method is proposed to effectively dispose of marine mud slurries. The advantages of this method are demonstrated herein in the following three aspects: dewatering performance, material savings, and the shear strength of the treated marine mud slurry. Then, the effects of the anionic polyacrylamide (APAM) dose, composite solidification agent dose, initial water content of marine mud slurries, and initial thickness of geo-bags on the mechanical properties of the marine mud slurry treated by the flocculation-solidification-high pressure filtration combined method are studied. Experimental results show that with increasing doses of APAM, the structures of mud slurries become more stable, and the optimal dose of APAM is determined as 0.16%. Moreover, the increase in the composite solidification agent dose and initial water content of the marine mud slurry, and the decrease in the initial thickness of geo-bags both contribute to the increase in the shear strength of the marine mud slurry treated by the flocculation-solidification-high pressure filtration combined method.



**Citation:** Han, C.; Xie, H.; Bai, B.; Zhang, R.; Gao, Y.; Zhao, Z. Experimental Study on Mechanical Properties of Marine Mud Slurry Treated by Flocculation-Solidification-High Pressure Filtration Combined Method. *J. Mar. Sci. Eng.* **2023**, *11*, 2270. <https://doi.org/10.3390/jmse11122270>

Academic Editors: José António Correia and José-Santos López-Gutiérrez

Received: 19 October 2023  
Revised: 15 November 2023  
Accepted: 28 November 2023  
Published: 29 November 2023



**Copyright:** © 2023 by the authors. Licensee MDPI, Basel, Switzerland. This article is an open access article distributed under the terms and conditions of the Creative Commons Attribution (CC BY) license (<https://creativecommons.org/licenses/by/4.0/>).

**Keywords:** marine mud slurry; flocculation; composite solidification agent; high-pressure filtration; shear strength

## 1. Introduction

In the projects of navigation construction, enormous amounts of marine mud slurry (MS) are hydraulically dredged from ports, harbors, and channels around the world [1]. Globally, several hundred million cubic meters of marine mud slurries with poor engineering characteristics are inevitably produced. For the massive quantities and negative impacts of dredged mud slurry, its disposal and utilization have become one of the most noticeable issues in the world [2–7]. Traditional solutions, such as inland deposits and ocean dumping, are increasingly unpopular for their deleterious influence on surroundings [8]. Considering the shortage of construction materials in civil engineering, a practically feasible solution is to convert large volumes of marine mud slurry into construction materials for reuse, such as embankment [9], subbase materials [10,11] and brick production [12]. Therefore, it is of great significance to investigate the efficient treatment and utilization of dredged marine mud slurry.

Scholars have demonstrated that the vacuum preloading method can significantly improve the mechanical properties of slurries [13–17]. The vacuum preloading method is used in the treatment of soft clays for the advantages of simple construction technology and low cost. However, the slurry has a high fine particle content and low permeability, and can easily block the drainage board. The vacuum preloading method has low drainage efficiency and long drainage times for slurry with high water content [18]. Furthermore,

the limited vacuum load inevitably results in the treated soil still belonging to soft soil, and can not directly convert marine mud slurry into filling material.

It has been widely accepted that the stabilization/solidification (S/S) techniques play a significant role in dredging sediments [19–22]. By adding a solidification agent, such as ordinary Portland cement (OPC), ground granulated blast furnace slag (GGBS) or metakaolin, the strength of slurries can be significantly increased [23]. Previous studies have gained a general understanding on the mechanism of sediment solidification [24]. It should be noted that the treatment efficiency of solidification agents on slurries is related to the water content. With the increase in water content, the curing efficiency of the solidification agent significantly decreases [25–27]. For marine mud slurry with high water content, the solidification treatment is either ineffective or extremely costly. The technique of flocculation and pressure of flocculated sediments is used in dewatering treatment of slurries. Flocculants have the function of promoting the dewatering rate of treated slurries [28,29]. Pressure filtration is a process of solid–liquid separation [30]. The mechanical properties of slurries treated by flocculation and pressure filtration will deteriorate after encountering water, making it difficult to reuse them.

In recent years, the combined physical and chemical method that integrates physical dewatering and chemical solidification has been proposed. This method can transform marine mud slurry into construction materials and apply them in reclamation, coastal embankment filling, and coastal slope protection [31]. However, as a new method, its fundamental principles and influencing factors are not well-understood. During the treatment process, the effects of the process parameters on the mechanical properties of the marine mud slurry are still unclear. This paper focuses on the flocculation-solidification-high pressure filtration combined method (FSHCM) to effectively process marine mud slurry. The effects of flocculant dose, composite solidification agent dose, initial water content and initial thickness of geo-bags on the mechanical properties of treated marine mud slurry are studied through laboratory experiments.

## 2. Laboratory Experiments

### 2.1. Materials

The materials employed in the experiments consisted of marine mud, solidification agent, and flocculants. The mud sample belonged to a marine deposit collected from an actual construction site located in Wenzhou, China. The basic physical and engineering properties of the mud sample are listed in Table 1.

**Table 1.** Basic properties of the marine mud slurries used in laboratory experiments.

Specific Density Gs	Liquid Limit $w_L$	Plastic Limit $w_p$	Plasticity Index	Organic Content (Ignition Loss) mo	Sand Fraction (0.075–2 mm)	Silt Fraction (0.002–0.075 mm)	Clay and Colloid Fraction (<0.002 mm)
2.69	56.1%	26.7%	29.4	4.41%	14.9%	79.5%	5.6%

The particle size of the mud was determined using a laser particle size analyzer, and the particle size distribution curve is shown in Figure 1. Based on the Unified Soil Classification System [32], the mud could be categorized as fat clay (CH). Additionally, the mud composition was analyzed using the 09 Empyrean X-ray diffractometer. This mud was composed of quartz, kaolinite, illite, smectite and mica. The composite solidification agents chosen for this experiment were the 425# OPC and GGBS. The flocculants used in the experiments were AN926SH anionic polyacrylamide (APAM) solution and  $\text{Ca}(\text{OH})_2$ . APAM is a widely employed substance in various industrial fields like water treatment, sludge dewatering, and the paper industry [33–35]. In this experiment, the APAM solution was prepared at a concentration of 1:500 (mass ratio of dry APAM powder to water). The APAM dose was defined as the dry weight ratio of APAM powder to the dry soil particles.  $\text{Ca}(\text{OH})_2$  can be consumed by GGBS; the hydration products improve the solidification effect [36].

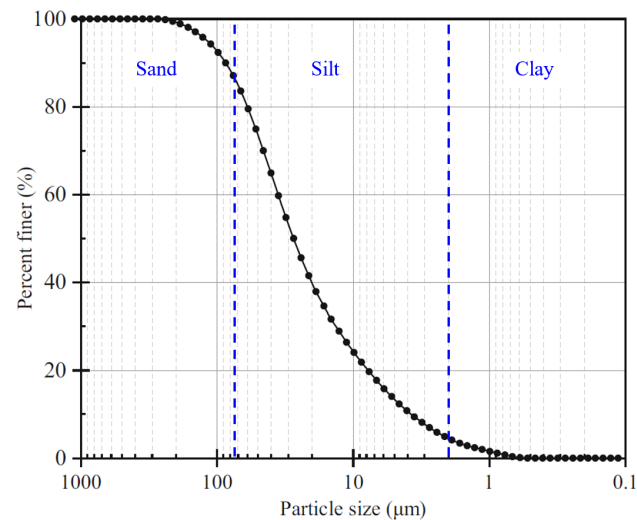


**Figure 1.** Particle size distribution curve for the mud sample.

## 2.2. Testing Procedures

The procedures of two types of tests, i.e., sedimentation tests and pressure filtration tests, are illustrated.

### (1) Sedimentation tests

Many scholars use settlement tests to investigate the sedimentation behavior of mud slurries [37–39], which provided a reference for our experiments. The detailed procedures for the sedimentation tests are listed below.

- (a) Set the initial dry weight of the mud sample (300 g) and the initial water content of the marine mud slurry (300%), and calculate the amount of experimental materials required.
- (b) Sequentially add water and  $\text{Ca}(\text{OH})_2$  to the marine mud slurry, and mix them at a constant speed using a multi-function mixer for 5 min. Then, manually stir the slurry for half a minute (to avoid insufficient mechanical mixing) to obtain a homogeneous slurry mixture.
- (c) Add the APAM solution to the slurry mixture and stir thoroughly to obtain a composite flocculant mixture.
- (d) Pour the composite flocculant mixture evenly into a 1.5 L capacity graduated cylinder, ensuring consistent initial liquid level height. In the initial stage of the experiment, record the sludge–water interface separation value every hour, and later, record it every 2 h until the value remains constant.

### (2) Pressure filtration tests

- (a) Use an electric agitator to uniformly mix the original marine mud slurry and take a sample to obtain its natural water content. Based on the natural water content of the mud slurry and the predetermined mix ratio, calculate the required masses of water,  $\text{Ca}(\text{OH})_2$ , OPC, and GGBS for the experiment.
- (b) Based on the calculation results from step (a), add the required amounts of water,  $\text{Ca}(\text{OH})_2$ , OPC, and GGBS sequentially to the slurry. Use a multifunctional mixer to thoroughly stir the slurry to obtain the mixture. The mixing process includes 5 min machine mixing in the beginning, 1 min hand mixing in the middle, and 3 min machine mixing in the end.
- (c) Add APAM solution to the slurry and use a stirring machine to mix it evenly. Slow down the stirring speed when agglomerates begin to form. Stop stirring when the supernatant liquid separates from the mixed slurry.
- (d) A specially developed device is used, as shown in Figure 2. This device is similar to a piston, through which the mud slurry can be dewatered, as demonstrated in the relevant standard [40]. Pour the mixed slurry into a geo-bag using a funnel and close

the zipper. Then, place the geo-bag in trough I and secure the cover plate on top of the pressure chamber using high-strength bolts. The material chosen for the geo-bags in this test was polypropylene fiber, which effectively prevents the seepage of mud particles and exhibits good permeability. The geo-bags had a planar dimension of 30 cm × 30 cm, and the maximum thickness was 20 cm. The aperture diameter of the geo-bags was 48 μm.

- (e) A hydraulic jack is used to apply pressure to the geo-bag and maintain the hydraulic pressure gauge reading at 15 MPa for 12 min. Observe the pressure gauge readings and control the pressure level accordingly.
- (f) Mud cake is obtained after the pressurization is completed. To ensure uniform initial water content for each sample, when taking samples with a ring cutter, avoid the edge of the mud cake. The samples are cylindrical, 61.8 mm in diameter and 20 mm in height. Place the sample into sealed bags and conduct the curing process. The curing temperature of the water bath incubator is  $20 \pm 3$  °C, and the curing ages are 7 days, 14 days, 21 days, and 28 days, respectively. After the samples reach the curing age, conduct water content tests and direct shear tests [41,42].

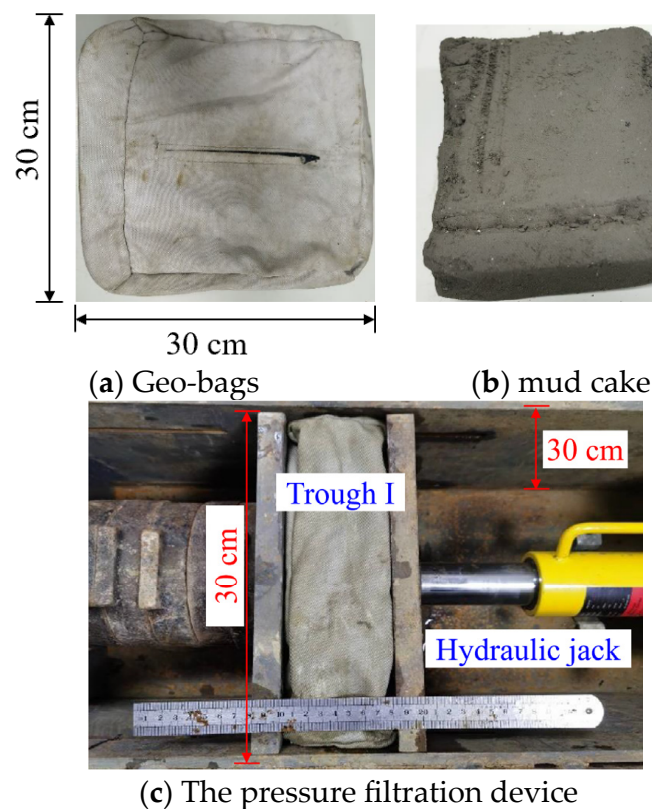


**Figure 2.** Pressure filtration tests.

### 2.3. Testing Program

The laboratory experiments included a total of 5 groups and 32 tests. Table 2 provides an overview of the mix proportions for all of these groups and tests. The curing conditions of samples for each group were the same. The curing temperature of the water bath incubator was  $20 \pm 3$  °C, and the curing ages were 7 days, 14 days, 21 days, and 28 days. The definitions of the symbols given in the table are as follows:  $w_{ei}$  represents the equivalent initial water content, defined as the ratio of the sum of the mass of water contained in the slurry itself and in the APAM solution to the mass of solids;  $M$  represents the dry weight of the slurry;  $C$  represents the dose of composite solidification agent (mass fraction).

**Table 2.** Program for the laboratory experiments.

Group	Test	w <sub>ei</sub> (%)	M (kg)	C (%)	APAM (%)	Ca(OH) <sub>2</sub> (%)
A	A1	200	2.5	6	0.16	1.5
	A2	200	0.3	0	0.16	1.5
	A3	200	2.5	20	0.16	1.5
B	B1	300	0.3	-	0	1.5
	B2	300	0.3	-	0.04	1.5
	B3	300	0.3	-	0.08	1.5
	B4	300	0.3	-	0.12	1.5
	B5	300	0.3	-	0.16	1.5
	B6	300	0.3	-	0.20	1.5
	B7	300	0.3	-	0.24	1.5
	B8	300	0.3	-	0.28	1.5
	B9	200	2.5	-	0	1.5
	B10	200	2.5	-	0.16	1.5
	B11	200	2.5	-	0.20	1.5
	B12	200	2.5	-	0.24	1.5
	B13	200	2.5	-	0.28	1.5
C	C1	200	2.5	3	0.16	1.5
	C2	200	2.5	5	0.16	1.5
	C3	200	2.5	7	0.16	1.5
	C4	200	2.5	9	0.16	1.5
D	D1	100	2.5	6	0.12	1.5
	D2	200	2.5	6	0.12	1.5
	D3	300	2.5	6	0.12	1.5
	D4	400	2.5	6	0.12	1.5
	D5	500	2.5	6	0.12	1.5
	D6	600	2.5	6	0.12	1.5
E	E1	200	2.5	6	0.16	1.5
	E2	200	3.0	6	0.16	1.5
	E3	200	3.5	6	0.16	1.5
	E4	200	4.0	6	0.16	1.5
	E5	200	4.5	6	0.16	1.5
	E6	200	5.0	6	0.16	1.5

Group A consisted of a feasibility exploration test for the FSHCM. This group included three tests (A1, A2 and A3) that adopted the FSHCM, flocculation-high pressure filtration combined method (FHCM), and flocculation-solidification combined method (FSCM), respectively. The feasibility of the FSHCM was verified by laboratory experiments. The strength of samples was obtained through direct shear tests. For each test, four samples were sheared under normal consolidation stresses of 50 kPa, 100 kPa, 150 kPa, and 200 kPa, respectively. The samples were cylindrical, 61.8 mm in diameter and 20 mm in height. The horizontal shear rate was set at 0.8 mm/min. In the three tests, the values of C were 0%, 6%, and 20%, respectively. A pressure filtration device was used in tests A1 and A2, with a pressure of 0.35 MPa and an action time of 12 min.

Group B included 13 tests with fixed w<sub>ei</sub> (B1~B8: 300%; B9~B13: 200%), M (0.3 kg), and Ca(OH)<sub>2</sub> dose (1.5%) but different APAM doses, varying from 0 to 0.28% (mass fraction). Sedimentation tests (B1~B8) and pressure filtration tests (B9~B13) were used to explore the effects of the APAM dose on the dewatering efficiency of FSHCM. The pressure and action time of the pressure filtration tests were the same as those of Group A.

The Group C tests explored the effects of the composite solidification agent dose on the shear characteristics of mud cake. The initial water content of the marine mud slurry was 200%, and the mass of dry soil was 2.5 kg. The doses (mass fraction) of Ca(OH)<sub>2</sub> and APAM were 1.5% and 0.16%, respectively. In the four tests in this group, the composite solidification agent doses were 3%, 5%, 7%, and 9% of the dry soil mass, respectively.

Group D included six tests, i.e., D1~D6, aiming to investigate the effects of initial water content on the shear characteristics of mud cake. The initial water contents of samples were 100%, 200%, 300%, 400%, 500%, and 600%, respectively.

Group E tests were conducted to study the effects of the initial thickness of geo-bags on the shear characteristics of mud cake. The initial thickness of geo-bags refers to the thickness of geo-bags when they were filled with mud slurries and placed in the pressure filtration device. The initial thickness of geo-bags included the thickness of the mud inserted in a geo-bag and the thickness of the geo-bag itself. This group involved five tests with different initial thicknesses of geo-bags (66 mm, 79 mm, 92 mm, 106 mm, 119 mm, and 132 mm).

### 3. Results and Discussion

#### 3.1. Feasibility Exploration Tests for the FSHCM

The experimental results of Group A are illustrated in this section to demonstrate the feasibility of FSHCM. Figure 3 depicts the relationship between water content and curing age for the mud samples treated using FSHCM, FHCM, and FSCM, respectively. When the curing age was less than 1 day, FSHCM had the best effect of dewatering, with the lowest sample water content. FHCM yielded a slightly higher water content compared to the former. FSCM, on the other hand, had the poorest effect of dewatering, with water contents significantly higher than those of the first two methods. FSHCM-MS, FHCM-MS, and FSCM-MS represent mud slurries treated by flocculation-solidification-high pressure filtration combined method, flocculation-high pressure filtration combined method, and flocculation-solidification combined method, respectively. When the curing age was longer than 1 day, the water content of FSHCM-MS decreased slowly. FHCM-MS showed almost no change in water content, while FSCM-MS exhibited a faster decrease in water content. The higher the dose of composite solidification agent, the more pore water was consumed by chemical reactions, resulting in a more significant decrease in the water content of the samples. FSHCM can reduce the water content of the marine mud slurry to a relatively low level through flocculation and high-pressure filtration. During the curing process, the water content of marine mud slurry is further decreased by the consumption of pore water. FSHCM has advantages both in terms of dewatering and material savings.

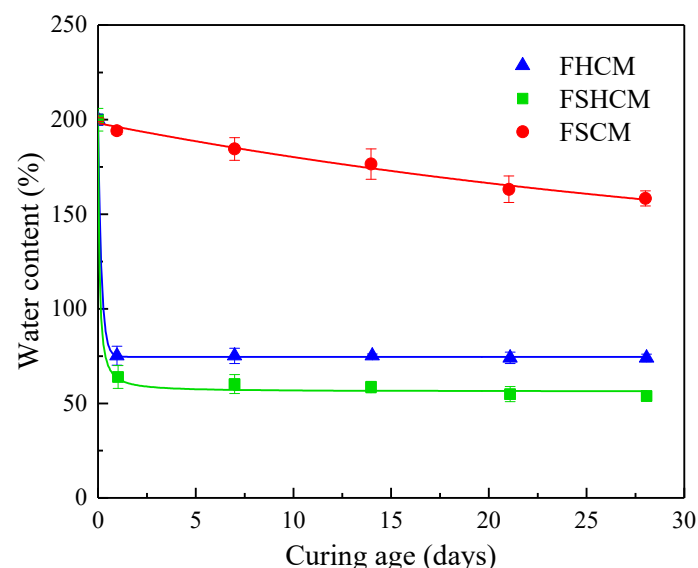


Figure 3. Relationship between water contents of mud samples and curing age.

Figure 4 illustrates the representative strength envelopes of samples treated by the three methods. It should be noted that the solid lines represent FSCM and the dashed lines represent FHCM in Figure 4b. With the increasing curing age, the shear strength envelopes of FSHCM-MS and FSCM-MS moved upward, indicating an increase in shear strength. Additionally, the shear strength envelope of FHCM-MS remained unchanged with curing

age. The shear strength envelope of FSHCM-MS at 7 days was located above the shear strength envelope of FSCM-MS at 28 days, indicating that FSHCM-MS achieved greater shear strength in a shorter time. Compared to FSCM, FSHCM needed less composite solidification agent, and FSHCM-MS achieved higher shear strength, demonstrating the efficiency of FSHCM.

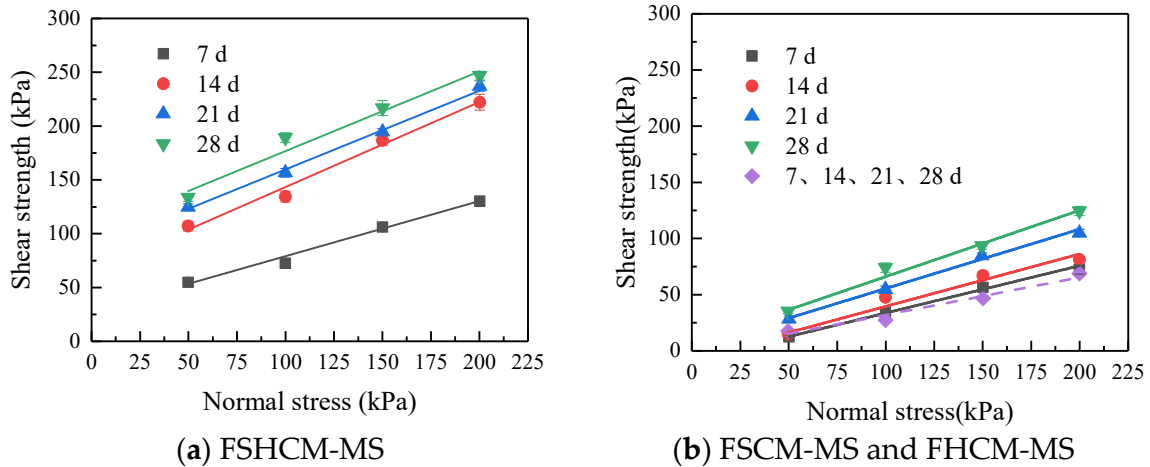


Figure 4. Strength envelopes of samples.

Figure 5 illustrates the effects of curing age on the cohesion and friction angle of samples treated by the three methods. It can be observed from Figure 5a that FHCM-MS exhibited no cohesion at 7 days, 14 days, 21 days, and 28 days of curing. This was attributed to the higher water content in FHCM-MS, which did not allow effective bonding between soil particles. FSCM-MS exhibited no cohesion at 7 days and 14 days of curing age, and it showed minimal cohesion at 21 days, which gradually increases with the curing period. After flocculation and dewatering treatment, there were still numerous pores between soil particles in the slurries. Under the influence of the composite solidification agent, it was challenging to establish effective bonds between soil particles in a short period. The cohesion of FSHCM-MS increased with curing age. Compared to FHCM-MS, the cohesion of FSHCM-MS increased by 104.89 kPa after 28 days of curing. Compared to FSCM-MS, FSHCM-MS saved 14% of the composite solidification agent dose and increased the cohesion by 94.59 kPa after 28 days of curing. From Figure 5b, it can be observed that the friction angle values for FSHCM-MS ranged from 20° to 38.5°, presenting significant advantages.

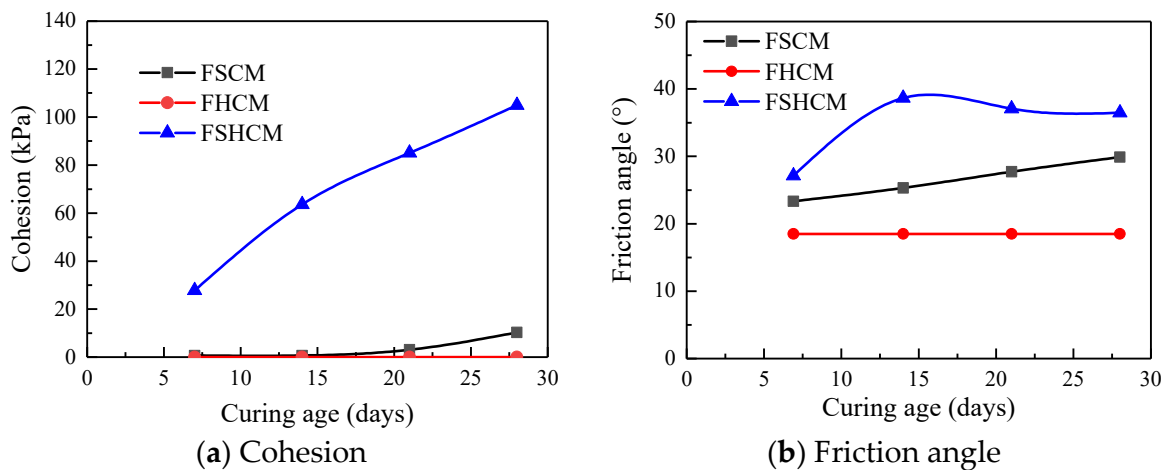


Figure 5. Effects of curing age on the cohesion and friction angle of samples.

### 3.2. Effects of APAM Dose on the Dewatering Performance of FSHCM-MS

In sedimentation tests, the mixed slurry was poured into a 1.5 L capacity graduated cylinder, and the supernatant liquid height,  $H_s$ , was recorded every 1 or 2 h. Figure 6 shows variation curves of  $H_s$  against time at various APAM doses. The same dose of  $\text{Ca}(\text{OH})_2$ , 1.5%, was adopted for all tests. As can be seen in Figure 6a, when the APAM content was 0%, 0.04%, 0.08% and 0.12%, the value of  $H_s$  increased significantly with time within 2000 min. The reason for this phenomenon is that the APAM dose was too small to form an effective flocculation structure between the clay particles. The mixed mud slurry was still a suspension.

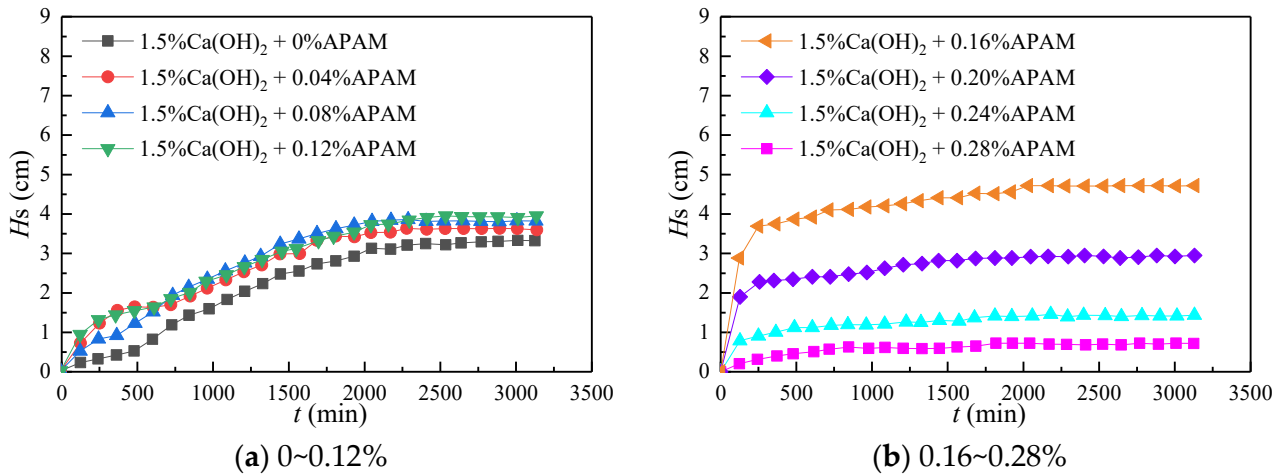


Figure 6. Variation curves of  $H_s$  against time at various APAM doses.

When the APAM dose was 0.16%, the value of  $H_s$  increased evidently, and the slope of the curve was larger within 200 min. Then, the curve entered a flatter state, and  $H_s$  approached a constant value after 2000 min, as shown in Figure 6b. As the APAM dose increases (0.20%, 0.24% and 0.28%), the  $H_s$  value gradually decreased, and the less time it took for the curve to reach a relatively stable state. The reason for this phenomenon is that with increasing APAM doses, the flocculation structure became larger, and the mixed slurry quickly approached a stable state. Therefore, a stable flocculation structure could be formed in the mud slurry when the APAM dose was 0.16%. As the APAM dose continued to increase, the flocculation structure became larger, the mixed slurry reached a stable state quickly, and the value of  $H_s$  changed less with time.

To investigate the effects of the APAM dose on the dewatering performance of FSHCM-MS, representative APAM doses (0%, 0.16%, 0.20%, 0.24%, and 0.28%) were selected for the analysis of the dewatering performance of the marine mud slurry. As shown in Figures 7 and 8, the mud cake without the addition of APAM was fragmented, and the filtrate was turbid. When APAM was added, the mud formed into a cake shape, and the filtrate was clear.

Figure 9 shows the effects of the APAM dose on the water content of the mud cake. When the APAM dose was 0.16%, the water content of the mud cake was only 65.56%. When APAM was not added, the water content of the mud cake was 150.6%, which was 2.3 times that of the mud cake without APAM, and the dewatering efficiency was significantly improved. Moreover, as the APAM dose increased, the water content of the mud cake decreased, but the rate became smaller.



(a) Without the addition of APAM (b) With the addition of APAM

Figure 7. Mud cake.



(a) Without the addition of APAM (b) With the addition of APAM

Figure 8. Filtrate.

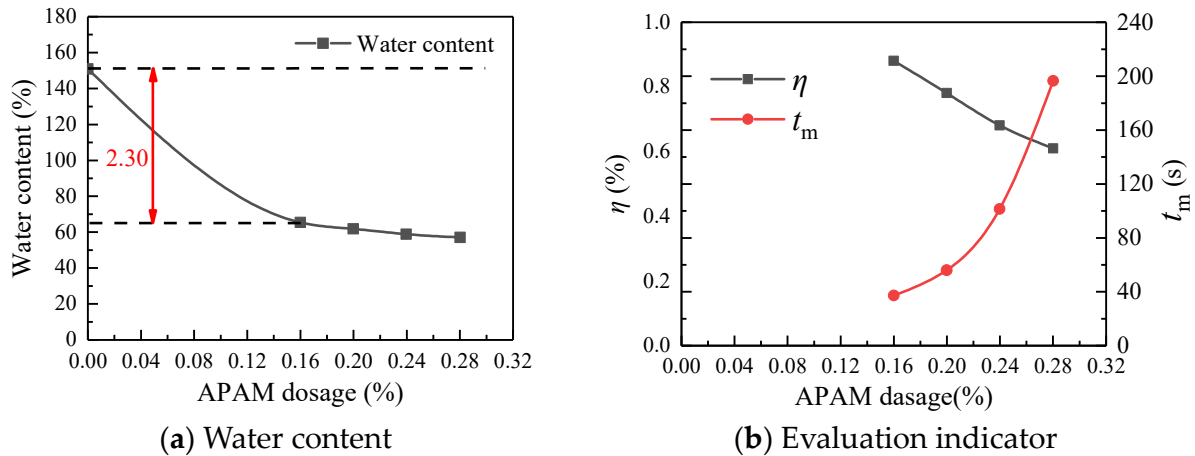


Figure 9. Effects of APAM dose on the water content and evaluation indicators.

The beneficial value of water consumption,  $\eta$ , was defined as shown in Equation (1). A smaller  $\eta$  value indicates a more significant wastage of water resources:

$$\eta = \frac{\omega_1 - \omega_2}{\omega_2} \times 100\% \tag{1}$$

where  $w_1$  represents the mass of drainage during the filtration process, and  $w_2$  represents the mass of water required to prepare the corresponding flocculant solution.

Additionally, mechanical stirring time was considered as another evaluation indicator. The mechanical stirring time was the mixing time of the agitator after adding the APAM

solution to the mud slurries. The shorter the mechanical stirring time, the greater the mud volume that could be processed per unit time. The effects of APAM dose on evaluation indicators are shown in Figure 9b. It can be observed that with an increase in APAM dose, the value of  $\eta$  exhibited a generally linear decrease, while the mechanical stirring time ( $t_m$ ), showed an exponential increase. The results indicate that as the APAM dose increased, the investment cost of FSHCM increased. Therefore, this study recommends an optimal APAM dose of 0.16%.

3.3. Effects of Composite Solidification Agent on the Shear Characteristics of FSHCM-MS

Figure 10 illustrates the effects of composite solidification agent dose on the water content of the mud cake. As seen in Figure 10a, the initial water content of the mud cake showed relatively small variations with changes in the dose of the composite solidification agent, and the dose of the composite solidification agent had little effect on the dewatering efficiency of the FSHCM. Figure 10b shows that with an increasing curing age, a higher solidification agent dose resulted in a faster decrease in the water content of the mud cake. For example, when the solidification agent dose was 3%, 5%, 7%, and 9%, the 28-day water content of the mud cake was 63.15%, 59.47%, 56.28%, and 52.84%, respectively.

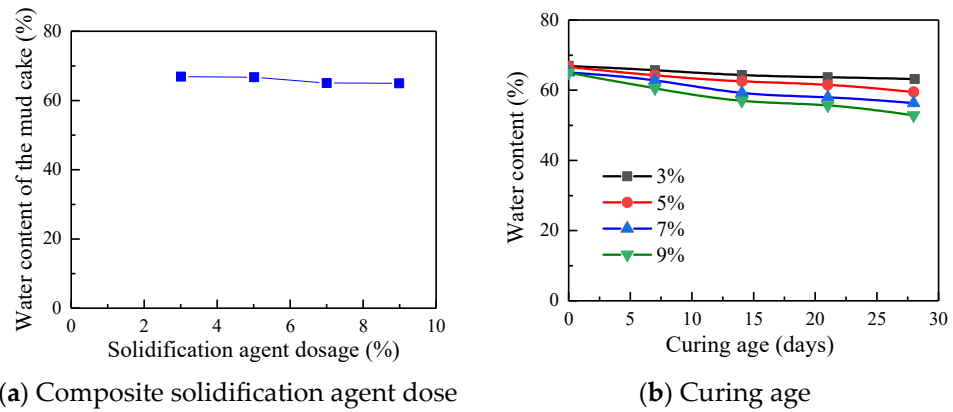


Figure 10. Effects of composite solidification agent dose on the water content of the mud cake.

Figure 11 illustrates the effects of the dose of the composite solidification agent on the shear strength of mud cakes. It can be observed from Figure 11a that samples with a higher dose of composite solidification agent had shear strength envelopes positioned above those with a lower dose. Under the same normal stress conditions, they exhibited greater shear strength.

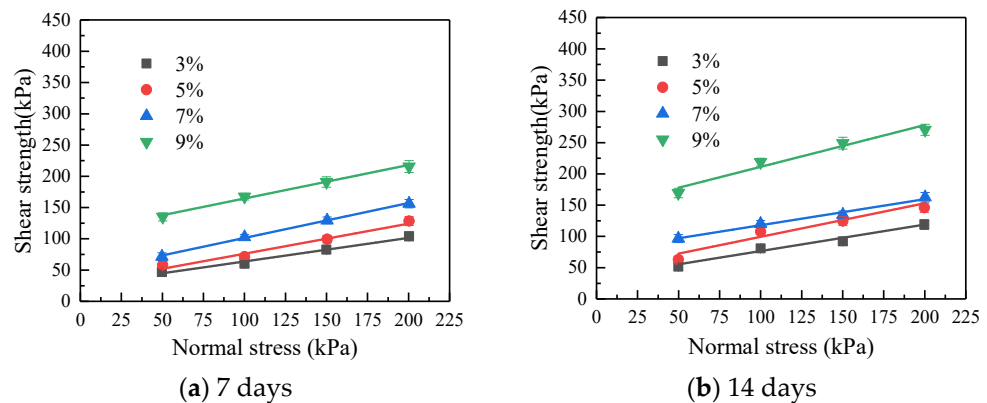


Figure 11. Cont.

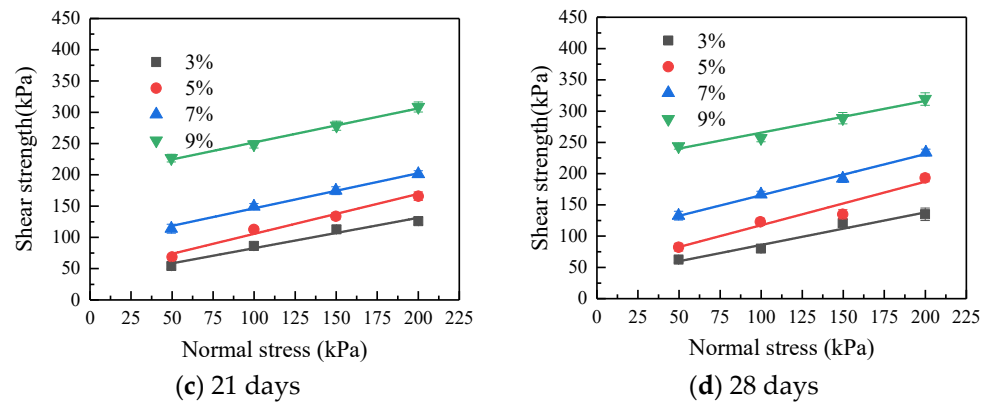


Figure 11. Shear strength envelopes.

Additionally, it is evident that with an increase in the dose of composite solidification agent, the spacing between the shear strength envelopes gradually increased. The spacing between the envelopes was notably larger for samples with a dose between 7% and 9%, suggesting that a higher dose of composite solidification agent leads to a greater increase in shear strength of the samples.

It can be observed from Figure 11 that the shear strength of the samples increased with the curing age. Using the experimental results with a normal force of 200 kPa as an example, when the samples were cured from 7 days to 28 days, the shear strength of the samples increased by 30.2 kPa, 64.12 kPa, 76.13 kPa, and 104.45 kPa, respectively, for composite solidification agent doses of 3%, 5%, 7%, and 9%. The higher the dose of the composite solidification agent, the faster the increase in the shear strength of the samples with curing age, and the greater the ultimate shear strength.

The Mohr–Coulomb criterion can be used in direct shear tests. Figure 12 illustrates the effects of the dose of the composite solidification agent on the cohesion and friction angle of the samples. As shown in Figure 12a, the cohesion of samples increased with curing age, and a higher dose of composite solidification agent resulted in a more pronounced increase in cohesion. For the same curing age, samples exhibited greater cohesion with a higher dose of composite solidification agent. As can be seen from Figure 12b, the values of the friction angle ranged between 20° and 35°.

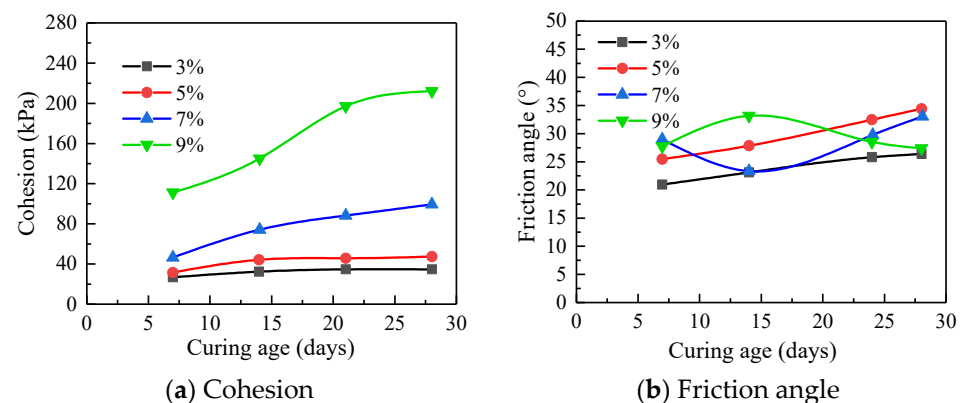
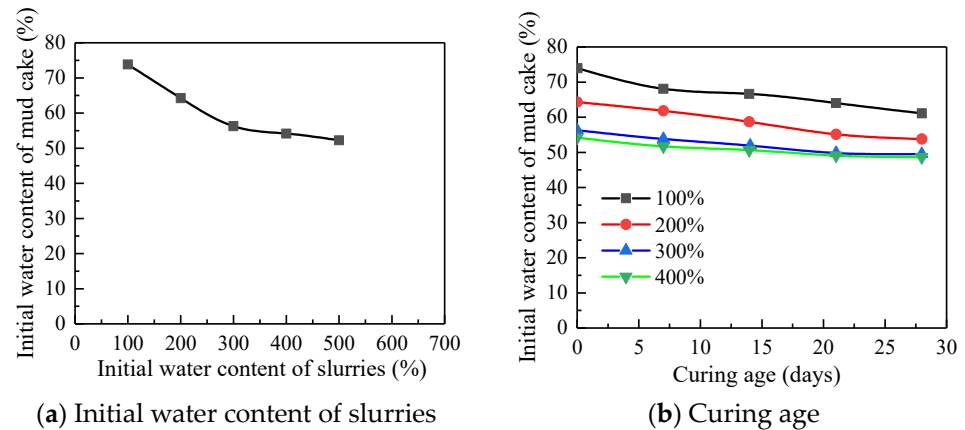


Figure 12. Effects of the dose of composite solidification agent on the cohesion and friction angle of samples.

### 3.4. Effects of Initial Water Content on the Shear Characteristics of FSHCM-MS

Figure 13 illustrates the effects of the initial water content of the marine mud slurry on the water content of the mud cake. As can be seen in Figure 13a, changing the initial water content of the marine mud slurry had a significant effect on the water content of the mud cake. As the initial water content of the marine mud slurry increased, the water

content of the mud cake decreased, and the rate of decrease became progressively smaller. When the initial water content of the marine mud slurry increased from 100% to 400%, the water content of the mud cake decreased by 19.6%. However, when the initial water content increased from 400% to 600%, the water content of the mud cake only decreased by 2.39%. During the experiment, it was observed that the higher the initial water content of the marine mud slurry, the larger the flocs formed by the flocculant, resulting in a faster sedimentation rate.



**Figure 13.** Effects of the initial water content of marine mud slurries on the initial water content of the mud cake.

It can be observed from Figure 13b that for a given dose of composite solidification agent, the higher the initial water content of the marine mud slurry, the lower the 28-day water content of the mud cake. Specifically, when the initial water content of the marine mud slurry was 100%, 200%, 300%, and 400%, the 28-day water content of the mud cake was 61.0%, 53.8%, 49.5%, and 48.7%, respectively. The reasons for this phenomenon include the following two points. The main reason is that as the initial water content of the marine mud slurry increased, there were fewer solid particles per unit volume, resulting in a higher initial porosity. This led to shorter drainage paths and higher drainage rates. Another possible reason is that the chosen APAM dose for this experiment (0.12%) was optimal for mud with high water content. At this dose, the dewatering performance was better in high-water-content samples compared to low-water-content samples.

Figure 14 illustrates the effects of the initial water content of the marine mud slurry on the shear strength of the mud cake. As can be seen from Figure 14a, it is evident that the shear strength envelope of the samples with a higher initial water content was positioned above that of the samples with a lower initial water content. This indicates that a higher initial water content of the marine mud slurry leads to greater shear strength of the filter-pressed mud cake under the same normal stress conditions.

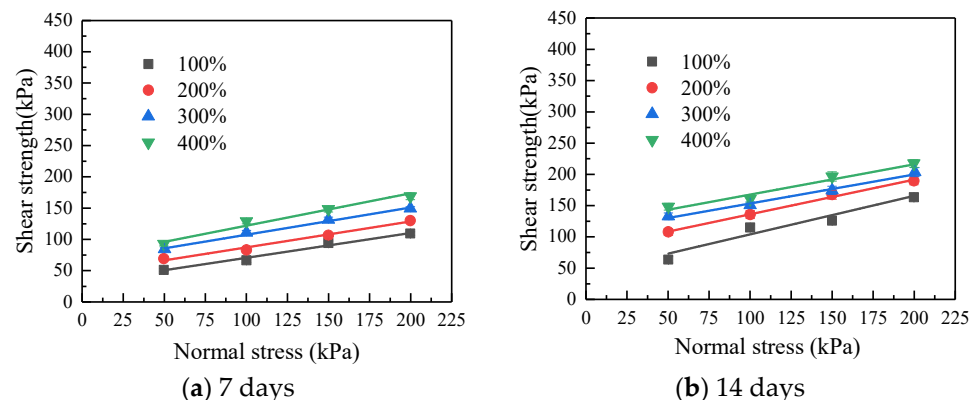


**Figure 14.** Cont.

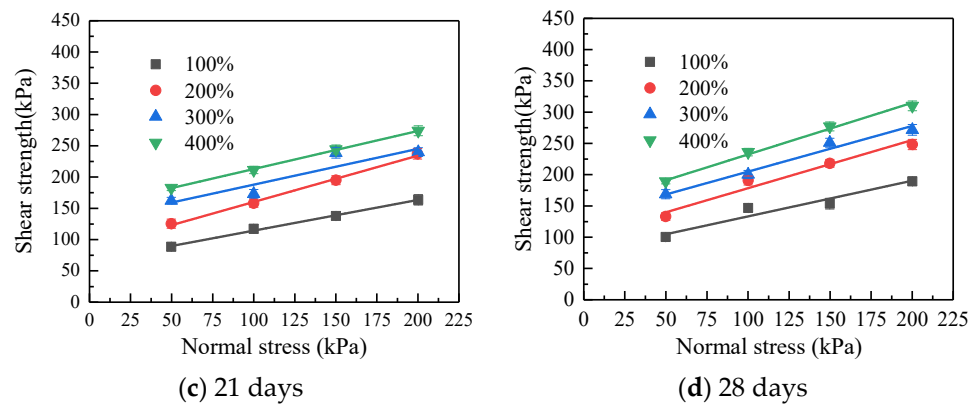


Figure 14. Shear strength envelopes.

Furthermore, the shear strength of the samples increased with curing age. Taking the normal stress of 200 kPa as an example, for samples cured from 7 days to 28 days, the shear strength increased as follows for the marine mud slurry with the initial water content of 100%, 200%, 300%, and 400%: 79.67 kPa, 117.77 kPa, 123.2 kPa, and 130.75 kPa, respectively. The higher the initial water content of the marine mud slurry, the faster the rate of increase in shear strength of the samples with curing age, resulting in a higher final shear strength value.

Figure 15 shows the effects of the initial water content of marine mud slurry on the cohesion and friction angle of mud cake. For slurries with the same initial water content, their cohesion increased with curing age. For mud cake cured from 7 days to 28 days, the cohesion of the samples increased as follows for the marine mud slurries with initial water contents of 100%, 200%, 300%, and 400%: 49.76 kPa, 60.58 kPa, 67.69 kPa, and 86.90 kPa, respectively. Moreover, a higher initial water content in the marine mud slurry led to greater cohesion of the samples. Figure 15b illustrates the curve of the friction angle of the samples with curing age. The values of the friction angle ranged between 20° and 35°.

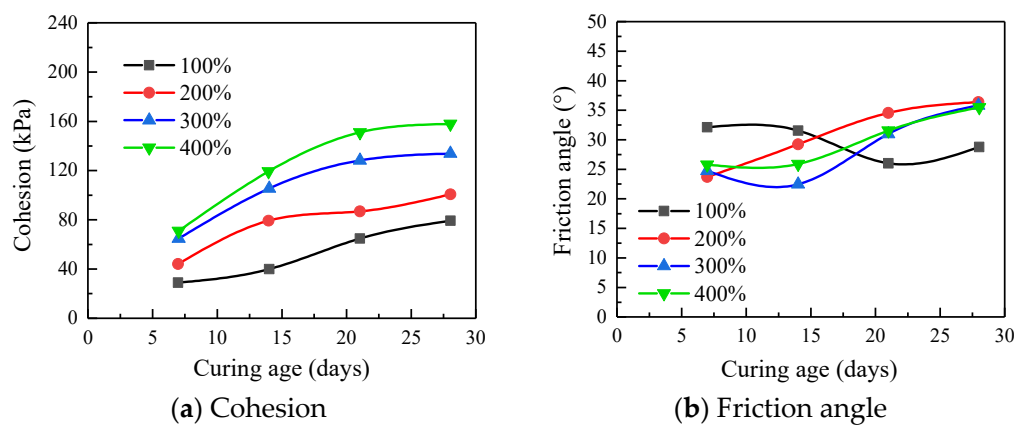


Figure 15. Effects of initial water content of marine mud slurries on the cohesion and friction angle of mud cake.

### 3.5. Effects of the Initial Thickness of Geo-Bags on the Shear Characteristics of FSHCM-MS

Figure 16 illustrates the effects of the initial thickness of the geo-bags on the initial water content of the mud cake. It can be observed from Figure 16a that as the initial thickness of the geo-bags increased, the initial water content of the mud cake remained relatively constant at first and then gradually increased. Specifically, the water content of the mud cake rose by 14.8% due to the increase in the initial thickness of the geo-bags from 92 mm to 132 mm, while it remained almost unchanged from 66 mm to 92 mm. Figure 16b illustrates the effects of the curing age on the water content of mud cake. When the same

dose of composite solidification agent was used, a smaller initial thickness of geo-bags resulted in a lower 28-day water content of the mud cake, mainly because the former led to shorter pore channels and better dewatering efficiency in the FSHCM.

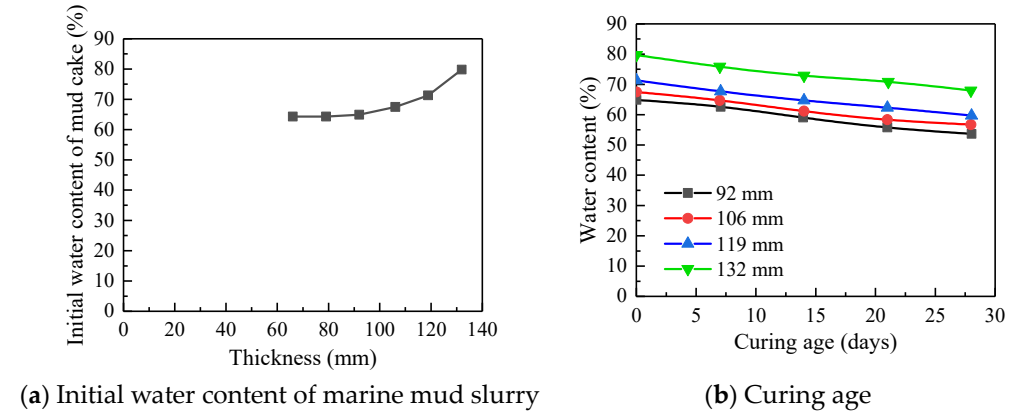


Figure 16. Effects of the initial thickness of geo-bags on the water content of the mud cake.

Figure 17 illustrates the effects of the initial thickness of geo-bags on the shear strength of the mud cake. It is obvious that the shear stress of the mud cake increases with increasing normal stress. Additionally, as shown in Figure 17a, the envelope of shear strength for mud cake with lower initial thickness of geo-bags was situated above that for mud cake with higher geo-bag thickness. This indicates that under the same normal stress conditions and curing age, a smaller initial thickness of geo-bags results in a larger shear strength of the mud cake. Taking a normal stress of 200 kPa as an example, the 7-day shear strength of the mud cake was 123.97 kPa, 118.59 kPa, 115.59 kPa, and 100.14 kPa for the thickness of 92 mm, 106 mm, 119 mm, and 132 mm, respectively.

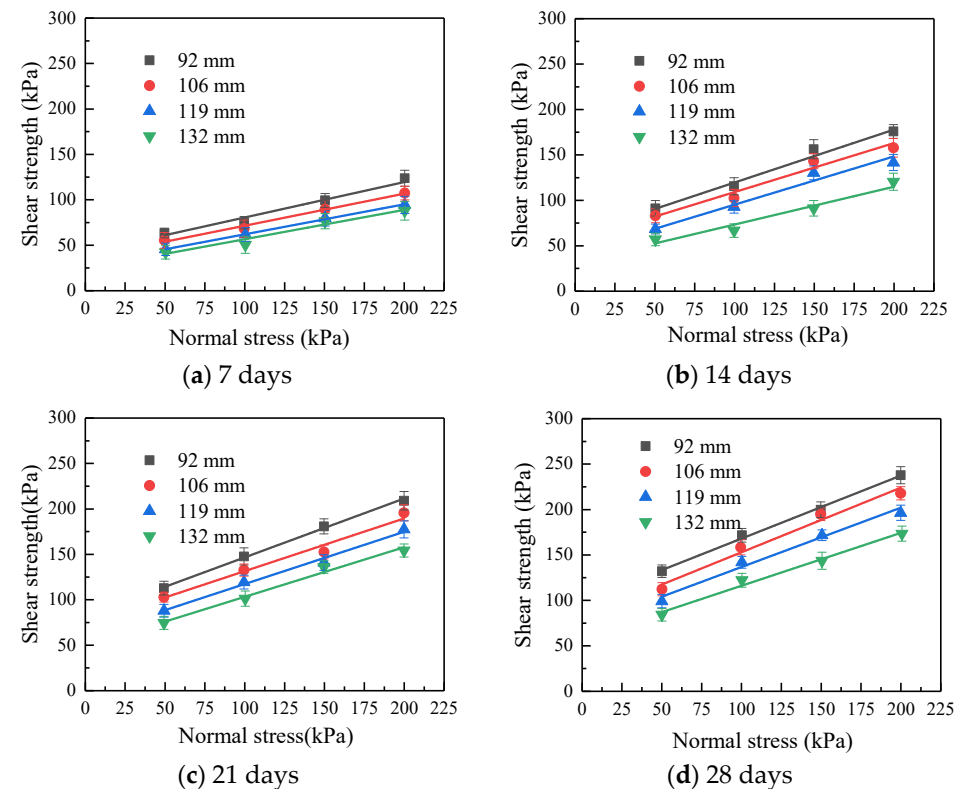
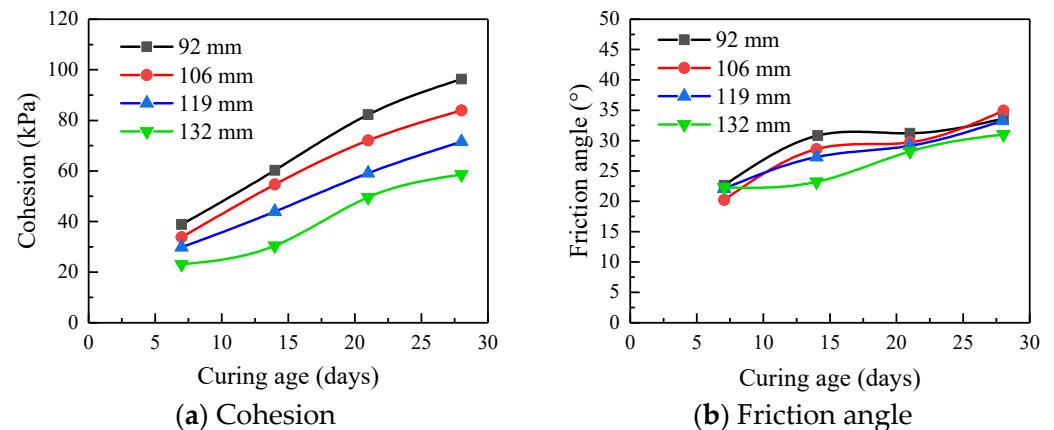


Figure 17. Shear strength envelopes.

Furthermore, with the increase in the curing age, the shear strength envelope gradually shifted upward, indicating that the shear strength of the mud cake increased with the curing age. Taking the normal stress of 200 kPa as an example, as the curing period increased from 7 days to 28 days, the shear strength of the samples increased by 114.48 kPa, 109.35 kPa, 92.2 kPa, and 74.86 kPa under the geo-bag thickness of 92 mm, 106 mm, 119 mm, and 132 mm, respectively. The results show that under the same normal force, the greater the initial thickness of the geo-bags, the smaller the increase in shear strength of mud cake with the change in curing period.

Figure 18 illustrates the effects of the initial thickness of the geo-bags on the cohesion and friction angle of the samples. As seen in Figure 18a, under the same curing age, a smaller thickness resulted in greater cohesion of the mud cake. Under the same geo-bag thickness, the cohesion of the mud cake increased with the increase in curing time. When the curing period increased from 7 days to 28 days, the cohesion of samples increased by 62.05 kPa, 51.79 kPa, 46.91 kPa, and 36.38 kPa under the geo-bag thickness of 92 mm, 106 mm, 119 mm, and 132 mm, respectively. Figure 18b depicts the variation in the friction angle. Under the same geo-bag thickness, the friction angle increased with the increase in curing age. The maximum value of the friction angle was 35°, and the minimum value was 20°.



**Figure 18.** Effects of the initial thickness of geo-bags on the cohesion and friction angle of the samples.

#### 4. Conclusions

In this study, a series of laboratory experiments were conducted to investigate the feasibility of FSHCM in marine mud slurries and the effects of APAM dose, composite solidification agent dose, the initial water content of marine mud slurries and the initial thickness of geo-bags on the mechanical properties of FSHCM-MS. The main conclusions are as follows:

1. Compared to the FHCM, the cohesion of the samples treated by the FSHCM decreased by 104.89 kPa at 28 days. Compared with FSCM, the FSHCM saved 14% of the composite solidification agent and increased cohesion by 94.59 kPa at 28 days. By comparing the water content and cohesion of mud cake treated by three methods, it was found that the FSHCM is more efficient.
2. When the APAM dose was 0.16%, FSHCM-MS exhibited a noticeable flocculation effect. As the APAM dose increased, the dewatering efficiency of FSHCM-MS improved. However, the water use efficiency value  $\eta$  decreased, and mechanical mixing time increased. Considering all factors, the optimal dose of APAM was determined as 0.16%.
3. The composite solidification agent dose had little effect on the dewatering efficiency of the FSHCM. The initial water content of the marine mud slurry had a significant effect on the dewatering efficiency of the combined method when it varied between 100% and 400%. Higher initial water content in the mud led to better dewatering

results. As the initial thickness of geo-bags increased, the initial water content of the mud cake remained constant at first, and then gradually increased.

4. An increase in composite solidification agent dose led to a higher rate of increase in the shear strength and cohesion of mud cake. As the initial water content of the marine mud slurry rose, the shear strength and cohesion of the mud cake increased. Moreover, an increase in the initial thickness of the geo-bags led to a decrease in the shear strength and cohesion of the mud cake.

**Author Contributions:** Conceptualization, C.H., H.X., B.B., R.Z. and Y.G.; methodology, C.H., H.X., R.Z. and Y.G.; validation, C.H., H.X. and B.B.; investigation, C.H., B.B., R.Z. and Y.G.; resources, C.H. and B.B.; data curation, H.X., B.B. and Y.G.; writing—original draft preparation, Z.Z., H.X. and C.H.; writing—review and editing, R.Z. and Y.G.; supervision, R.Z.; funding acquisition, C.H., H.X. and B.B. All authors have read and agreed to the published version of the manuscript.

**Funding:** This research was funded by the Science and Technology Project of State Grid Jiangsu Electric Power Co., Ltd. (Grant No. J2021047).

**Institutional Review Board Statement:** Not applicable.

**Informed Consent Statement:** Not applicable.

**Data Availability Statement:** All data have been provided in the paper.

**Conflicts of Interest:** Authors Chao Han, Hongping Xie, and Bin Bai were employed by the Construction Branch of State Grid Jiangsu Electric Power Co., Ltd. The remaining authors declare that the research was conducted in the absence of any commercial or financial relationships that could be construed as a potential conflict of interest.

## References

1. Chrysochoou, M.; Grubb, D.G.; Drenkler, K.L.; Malasavage, N.E. Stabilized Dredged Material. III: Mineralogical Perspective. *J. Geotech. Geoenviron. Eng.* **2010**, *136*, 1037–1050. [[CrossRef](#)]
2. Xu, G.; Gao, Y.; Hong, Z.; Ding, J. Sedimentation behavior of four dredged slurries in China. *Mar. Georesour. Geotechnol.* **2012**, *30*, 143–156. [[CrossRef](#)]
3. Zeng, L.; Hong, Z.; Tian, W.; Shi, J. Settling behavior of clay suspensions produced by dredging activities in China. *Mar. Georesour. Geotechnol.* **2018**, *36*, 30–37. [[CrossRef](#)]
4. Wang, S.Y.; Fu, J.Y.; Zhang, C.; Yang, J.S. *Shield Tunnel Engineering, Chapter 10 Slurry Treatment for Shield Tunnelling and Waste Slurry Recycling*; Elsevier: Amsterdam, The Netherlands, 2021. [[CrossRef](#)]
5. Foged, S.; Duerinckx, L.; Vandekeybus, J. An innovative and sustainable solution for sediment disposal problems. In Proceedings of the Eighteenth World Dredging Congress, Lake Buena Vista, FL, USA, 27 May–1 June 2007; pp. 1513–1528.
6. Spadaro, P.; Rosenthal, L. River and harbor remediation: “polluter pays,” alternative finance, and the promise of a “circular economy”. *J. Soils Sediments* **2020**, *20*, 4238–4247. [[CrossRef](#)]
7. Hussan, A.; Levacher, D.; Mezazigh, S. Investigation of natural dewatering of dredged sediments incorporating evaporation and drainage. *Dry. Technol.* **2023**, *41*, 2227–2240. [[CrossRef](#)]
8. Sheehan, C.; Harrington, J. Management of dredge material in the Republic of Ireland—A review. *Waste Manag.* **2012**, *32*, 1031–1044. [[CrossRef](#)] [[PubMed](#)]
9. Levacher, D.; Sanchez, M. Characterization of marine sediments for a reuse in land disposal and embankment. *Eur. J. Environ. Civ. Eng.* **2011**, *15*, 167–178. [[CrossRef](#)]
10. Zentar, R.; Dubois, V.; Abriak, N.E. Mechanical behaviour and environmental impacts of a test road built with marine dredged sediments. *Resour. Conserv. Recycl.* **2008**, *52*, 947–954. [[CrossRef](#)]
11. Achour, R.; Abriak, N.-E.; Zentar, R.; Rivard, P.; Gregoire, P. Valorization of unauthorized sea disposal dredged sediments as a road foundation material. *Environ. Technol.* **2014**, *35*, 1997–2007. [[CrossRef](#)]
12. Samara, M.; Lafhaj, Z.; Chapiseau, C. Valorization of stabilized river sediments in fired clay bricks: Factory scale experiment. *J. Hazard. Mater.* **2009**, *163*, 701–710. [[CrossRef](#)]
13. Sun, L.; Gao, X.; Zhuang, D.; Guo, W.; Hou, J.; Liu, X. Pilot tests on vacuum preloading method combined with short and long PVDs. *Geotext. Geomembr.* **2018**, *46*, 243–250. [[CrossRef](#)]
14. Sun, H.; Weng, Z.; Liu, S.; Geng, X.; Pan, X.; Cai, Y.; Shi, L. Compression and consolidation behaviors of lime-treated dredging slurry under vacuum pressure. *Eng. Geol.* **2020**, *270*, 105573. [[CrossRef](#)]
15. Wang, J.; Ni, J.; Cai, Y.; Fu, H.; Wang, P. Combination of vacuum preloading and lime treatment for improvement of dredged fill. *Eng. Geol.* **2017**, *227*, 149–158. [[CrossRef](#)]
16. Wang, J.; Cai, Y.; Ma, J.; Chu, J.; Fu, H.; Wang, P.; Jin, Y. Improved vacuum preloading method for consolidation of dredged clay-slurry fill. *J. Geotech. Geoenviron. Eng.* **2016**, *142*, 06016012. [[CrossRef](#)]

17. Zhou, Y.; Cai, Y.; Yuan, G.; Wang, J.; Fu, H.; Hu, X.; Geng, X.; Li, M.; Liu, J.; Jin, H. Effect of tamping interval on consolidation of dredged slurry using vacuum preloading combined with dynamic consolidation. *Acta Geotech.* **2021**, *16*, 859–871. [[CrossRef](#)]
18. Cui, Y.; Pan, F.; Zhang, B.; Wang, X.; Diao, H. Laboratory test of waste mud treated by the flocculation-vacuum-curing integrated method. *Constr. Build. Mater.* **2022**, *328*, 127086. [[CrossRef](#)]
19. Boutouil, M. Traitement des Vases de Dragage par Stabilisation/Solidification à Base de Ciment et Additifs (Treatment of Dredging Muds by Stabilization/Solidification with Cement and Additives). Ph.D. Thesis, University of Le Havre, Le Havre, France, 1998.
20. Lahtinen, P.; Forsman, J.; Kiukkonen, P.; Kreft-Burman, K.; Niutanen, V. Mass stabilisation as a method of treatment of contaminated sediments. In Proceedings of the South Baltic Conference on Dredged Materials in Dike Construction, Rostock, Germany, 10–12 April 2014; pp. 145–155.
21. Lirer, S.; Liguori, B.; Capasso, I.; Flora, A.; Caputo, D. Mechanical and chemical properties of composite materials made of dredged sediments in a fly-ash based geopolymer. *J. Environ. Manag.* **2017**, *191*, 1–7. [[CrossRef](#)]
22. Yoobanpot, N.; Jamsawang, P.; Poorahong, H.; Jongpradist, P.; Likitlersuang, S. Multiscale laboratory investigation of the mechanical and microstructural properties of dredged sediments stabilized with cement and fly ash. *Eng. Geol.* **2020**, *267*, 105491. [[CrossRef](#)]
23. Horpibulsuk, S.; Rachan, R.; Suddeepong, A. Assessment of strength development in blended cement admixed Bangkok clay. *Constr. Build. Mater.* **2011**, *25*, 1521–1531. [[CrossRef](#)]
24. Sollars, C.; Perry, R. Cement-based stabilization of wastes: Practical and theoretical considerations. *Water Environ. J.* **1989**, *3*, 125–134. [[CrossRef](#)]
25. Yamashita, E.; Cikmit, A.A.; Tsuchida, T.; Hashimoto, R. Strength estimation of cement-treated marine clay with wide ranges of sand and initial water contents. *Soils Found.* **2020**, *60*, 1065–1083. [[CrossRef](#)]
26. Vu, M.C.; Satomi, T.; Takahashi, H. Influence of initial water, moisture, and geopolymer content on geopolymer modified sludge. *Constr. Build. Mater.* **2020**, *235*, 117420. [[CrossRef](#)]
27. Su, Y.; Luo, B.; Luo, Z.; Xu, F.; Huang, H.; Long, Z.; Shen, C. Mechanical characteristics and solidification mechanism of slag/fly ash-based geopolymer and cement solidified organic clay: A comparative study. *J. Build. Eng.* **2023**, *71*, 106459. [[CrossRef](#)]
28. Arjmand, R.; Massinaei, M.; Behnamfard, A. Improving flocculation and dewatering performance of iron tailings thickeners. *J. Water Process Eng.* **2019**, *31*, 100873. [[CrossRef](#)]
29. Maraschin, M.; Ferrari, K.F.H.; Carissimi, E. Acidification and flocculation of sludge from a water treatment plant: New action mechanisms. *Sep. Purif. Technol.* **2020**, *252*, 117417. [[CrossRef](#)]
30. Wakeman, R.; Tarleton, S. *Solid/Liquid Separation: Principles of Industrial Filtration*; Elsevier: Amsterdam, The Netherlands, 2005.
31. Zhang, R.; Dong, C.; Lu, Z.; Pu, H. Strength characteristics of hydraulically dredged mud slurry treated by flocculation-solidification combined method. *Constr. Build. Mater.* **2019**, *228*, 116742. [[CrossRef](#)]
32. ASTM D2487-11; Standard Practice for Classification of Soils for Engineering Purposes (Unified Soil Classification System). ASTM International: West Conshohocken, PA, USA, 2017.
33. Amuda, O.; Amoo, I. Coagulation/flocculation process and sludge conditioning in beverage industrial wastewater treatment. *J. Hazard. Mater.* **2007**, *141*, 778–783. [[CrossRef](#)] [[PubMed](#)]
34. Jin, L.; Zhang, P.; Zhang, G.; Li, J. Study of sludge moisture distribution and dewatering characteristic after cationic polyacrylamide (C-PAM) conditioning. *Desalin Water Treat.* **2016**, *57*, 29377–29383. [[CrossRef](#)]
35. Kang, J.; McLaughlin, R.A. Simple systems for treating pumped, turbid water with flocculants and a geotextile dewatering bag. *J. Environ. Manag.* **2016**, *182*, 208–213. [[CrossRef](#)]
36. Preetham, H.; Nayak, S. Geotechnical investigations on marine clay stabilized using granulated blast furnace slag and cement. *Int. J. Geosynth. Groun* **2019**, *5*, 28. [[CrossRef](#)]
37. Bertrand, G.; Roy, P.; Filiatre, C.; Coddet, C. Spray-dried ceramic powders: A quantitative correlation between slurry characteristics and shapes of the granules. *Chem. Eng. Sci.* **2005**, *60*, 95–102. [[CrossRef](#)]
38. Du, Y.; Yang, Y.; Fan, R.; Wang, F. Effects of phosphate dispersants on the liquid limit, sediment volume and apparent viscosity of clayey soil/calcium-bentonite slurry wall backfills. *KSCE J. Civ. Eng.* **2016**, *20*, 670–678. [[CrossRef](#)]
39. He, J.; Chu, J.; Tan, S.K.; Vu, T.T.; Lam, K.P. Sedimentation behavior of flocculant-treated soil slurry. *Mar. Georesour. Geotechnol.* **2017**, *35*, 593–602. [[CrossRef](#)]
40. EN 14701-2:2013 (E); Characterisation of Sludges-Filtration Properties-Part 2: Determination of the Specific Resistance to Filtration. CEN—UNI EN: Brussels, Belgium, 2013.
41. ASTM D2216-19; Standard Test Methods for Laboratory Determination of Water (Moisture) Content of Soil and Rock by Mass. ASTM International: West Conshohocken, PA, USA, 2019.
42. ASTM D7702/D7702M-14; Standard Guide for Considerations When Evaluating Direct Shear Results Involving Geosynthetics. ASTM International: West Conshohocken, PA, USA, 2021.

**Disclaimer/Publisher’s Note:** The statements, opinions and data contained in all publications are solely those of the individual author(s) and contributor(s) and not of MDPI and/or the editor(s). MDPI and/or the editor(s) disclaim responsibility for any injury to people or property resulting from any ideas, methods, instructions or products referred to in the content.